Journal of Applied Electrochemistry **31**: 1163–1170, 2001.

Reliability and accuracy of measured overpotential in a three-electrode fuel cell system

S.H. CHAN, X.J. CHEN and K.A. KHOR
Fuel Cell Technology Strategic Research Programme, School of Mechanical and Production Engineering, Nanyang Technological University, 50 Nanyang Avenue, Singapore 639798

Received 6 February 2001; accepted in revised form 12 June 2001

Key words: fuel cell, measurement error, potential and current distribution, three-electrode system measurement

Abstract

Numerical simulation was conducted to study the potential and current density distributions at the active electrode surface of a solid oxide fuel cell. The effects of electrode deviation, electrolyte thickness and electrode polarization resistance on the measurement error were investigated. For a coaxial anode/electrolyte/cathode system where the radius of the anode is greater than that of cathode, the cathode overpotential is overestimated while the anode overpotential is underestimated. Although the current interruption method or impedance spectroscopy can be employed to compensate/correct the error for a symmetric electrode configuration, it is not useful when dealing with the asymmetric electrode system. For the purpose of characterizing the respective overpotentials in a fuel cell, the cell configuration has to be carefully designed to minimize the measurement error, in particular the selection of the electrolyte thickness, which may cause significant error. For the anode-support single fuel cell, it is difficult to distinguish the polarization between the anode and cathode with reference to a reference electrode. However, numerical results can offer an approximate idea about the source/cause of the measurement error and provide design criteria for the fuel cell to improve the reliability and accuracy of the measurement technique.

List of symbols

F	faradaic constant
i	current density (A cm^{-2})
i_o	exchange current density (A cm^{-2})
L	thickness of the electrode (cm)
R	gas constant
R^A_{app}	area specific polarization resistance (Ω cm^2)
S^*	active area per unit volume (cm^2 cm^{-3})
T	temperature (K)
E_o	equilibrium voltage of the cell (V)
E	output voltage of the cell (V)
U	applied voltage (V)

Greek symbols

η	microoverpotential within the electrode (V)
η_{obs}	observed overpotential of the total electrode without ohmic compensation (V)
η_{app}	apparent overpotential of the total electrode with ohmic compensation (V)
α, β	transfer coefficient
φ	electrode potential (V)
ϕ	absolute inner potential of the electrolyte (V)

Subscripts

A	anode
C	cathode
RE	reference electrode
obs	observed
app	apparent
a	assumed
e	electrolyte phase
eq	equilibrium condition
Ox	oxidant
Re	reductant
io	ionic conductor
el	electronic conductor

Superscripts

eff	effective
A	area-specific polarization resistance

1. Introduction

To study the performance of solid oxide fuel cell (SOFC), the respective polarization of cell electrodes should be determined independently and accurately [1–3]. It is impractical to measure the absolute potential difference across an electrode–electrolyte interface since each attempt to do so will inevitably introduce a new

electrode–electrolyte interface. Generally, a reference electrode is used to make relative measurement possible, such as the use of the normal hydrogen electrode (NHE) whose potential is defined as zero. In SOFC research, the platinum electrode is used exclusively as the reference electrode to measure the anodic and cathodic polarization. The criteria for reference selection include: (i) the reference electrode should be a reversible electrode which obeys the Nernst Equation, (ii) the electrode potential should be stable, and (iii) the electrode should be able to respond quickly to changes in environmental conditions.

Newman [4] calculated the current distribution on a rotating disc electrode below the limiting current and concluded that the non-uniform ohmic drop between the rotating disc electrode and the reference electrode can lead to errors in determining the kinetic parameters. West and Newman [5, 6] proposed an analysis procedure to correct the kinetic measurements taken from a disk electrode. The importance of reference electrode location in the overpotential measurement of a single fuel cell with yttria-stablized zirconia (YSZ) electrolyte was studied by Nagata et al. [7]. Winkle [8] et al. studied the measurement errors of a geometrically different three-electrode configuration. The influence of cell configuration on interfacial impedance measurement with three electrodes was investigated by Kato et al. [9]. It was concluded that the difference in diameter between the working electrode and the counter electrode could introduce significant experimental error, causing deformed impedance spectra from a simple semicircle. Adler et al. [10] also reported that misalignment of axes of electrodes on a thin electrolyte could wreak havoc on electrochemical measurements.

Although a.c. impedance spectroscopy is commonly used to study reaction kinetics, the traditional electrochemical measurement of the η/i curve is still a powerful technique to determine the kinetic parameters under operating conditions. A porous electrode can be visualized as a multilayered slab with uniformly distributed reaction zones laid across the electrode. Within each reaction layer, the charge transfer between the electronic and ionic conductors can be written in a general form of Butler–Volmer expression:

$$i = i_{\mathrm{o}}\left\{\frac{C_{\mathrm{Ox}}}{C^{0}_{\mathrm{Ox}}}\exp\left(\frac{\alpha F}{RT}\eta\right) - \frac{C_{\mathrm{Re}}}{C^{0}_{\mathrm{Re}}}\exp\left(-\frac{\beta F}{RT}\eta\right)\right\} \qquad (1)$$

In the low overpotential case, the concentration of oxidant and reductant remains almost constant along the thickness of the electrode, that is $C_{\mathrm{Ox}} = C^{0}_{\mathrm{Ox}}, C_{\mathrm{Re}} = C^{0}_{\mathrm{Re}}$. Taking $\alpha = \beta = 0.5$, $T = 1273$ K and $\eta < 0.1$ V, yields $\alpha F\eta/RT < 0.5$. In this case, the Butler–Volmer equation can be approximated by the linear current–potential expression with an error lower than 4%. Paola et al. [11] developed a micromodel for SOFC porous electrodes based on this linear assumption. In their model, the apparent electrode overpotential is expressed as

$$\eta_{\mathrm{app}} = \frac{iL(\rho^{\mathrm{eff}}_{\mathrm{io}} + \rho^{\mathrm{eff}}_{\mathrm{el}})}{\Gamma\sinh(\Gamma)} \times \{\cosh(\Gamma) + \Omega[2 + \sinh(\Gamma) - 2\cosh(\Gamma)]\} \qquad (2)$$

where $\Omega = \dfrac{\rho^{\mathrm{eff}}_{\mathrm{io}}\rho^{\mathrm{eff}}_{\mathrm{el}}}{\rho^{\mathrm{eff}}_{\mathrm{io}} + \rho^{\mathrm{eff}}_{\mathrm{el}}}$ and $\Gamma^2 = \dfrac{i_{\mathrm{o}}S^{*}F(\rho^{\mathrm{eff}}_{\mathrm{io}} + \rho^{\mathrm{eff}}_{\mathrm{el}})L^2}{RT}$

or

$$\eta_{\mathrm{app}} = R^{\mathrm{A}}_{\mathrm{app}} \times i \qquad (3)$$

where

$$R^{\mathrm{A}}_{\mathrm{app}} = \frac{L(\rho^{\mathrm{eff}}_{\mathrm{io}} + \rho^{\mathrm{eff}}_{\mathrm{el}})}{\Gamma\sinh(\Gamma)} \times \{\cosh(\Gamma) + \Omega[2 + \sinh(\Gamma) - 2\cosh(\Gamma)]\}$$

The area-specific polarization resistance ($R^{\mathrm{A}}_{\mathrm{app}}$) of SOFC electrodes varies from the perovskite cathode or cermet anode of about 0.1 $\Omega\,\mathrm{cm}^2$ to the platinum electrode of about 10 $\Omega\,\mathrm{cm}^2$. The magnitude of this apparent resistance is closely related to the specifications of the raw materials used the electrical properties of the electrodes, fabrication techniques, sintering and operating temperatures. In this study, it is assumed that the area-specific polarization resistance of the anode and cathode is equal to 0.2 $\Omega\,\mathrm{cm}^2$.

In view of the importance of the reliability/accuracy of the measured overpotential in reflecting the true performance of an electrode, the authors focus on the study of the effects of electrode properties, cell configuration and reference position on the steady-state polarization. In this study, an electrical conduction model of the electrolyte has been developed and solved by a finite difference method. The computed results would provide valuable design criteria for laboratory-scaled fuel cells to minimize the measurement errors.

2. General description of the test fuel cell

If an electrolyte has homogeneous composition and constant conductivity, ionic transport should obey the Laplace equation:

$$\nabla^2\phi = 0 \qquad (4)$$

When impedance spectroscopy or the current interruption method is used to compensate the ohmic loss between the working and reference electrode, the current and potential distribution within the electrolyte is known as the primary distribution [12]. In this context, the associated boundary conditions for the Laplace equation are:

$$\phi_{\mathrm{A}} = U \quad \text{for electrolyte surface covering the anode, } \Gamma_{\mathrm{A}} \qquad (5)$$

$$\phi_C = 0 \quad \text{for electrolyte surface covering the cathode, } \Gamma_C \tag{6}$$

$$\frac{\partial \phi}{\partial \vec{n}} = 0 \quad \text{for electrolyte surface without covering the electrode, } \Gamma_\Omega \tag{7}$$

where ϕ is the absolute inner potential of the electrolyte, U is the applied voltage and the subscript A, C refer to the anode and cathode, respectively.

If the electrodes are connected to an electrical load, R, and in which case the electrode overpotential cannot be neglected, the current and potential distribution within the electrolyte is known as the secondary distribution. The boundary conditions for the Laplace equation under polarization are:

$$\phi_A = E_o - E - \eta_A \quad \text{for electrolyte surface covering the anode, } \Gamma_A \tag{8}$$

$$\phi_C = \eta_C \quad \text{for electrolyte surface covering the cathode, } \Gamma_C \tag{9}$$

$$\frac{\partial \phi}{\partial \vec{n}} = 0 \quad \text{for electrolyte surface without covering the electrode, } \Gamma_\Omega \tag{10}$$

where E_o is equilibrium voltage of the cell, E is the output voltage of the cell, η_A and η_C are the overpotentials of the anode and cathode, respectively.

Because of the non-uniformity of current distribution due to polarization at the surfaces of anode and cathode, the overpotentials of these electrodes and the boundary conditions are all a function of radius (r coordinate).

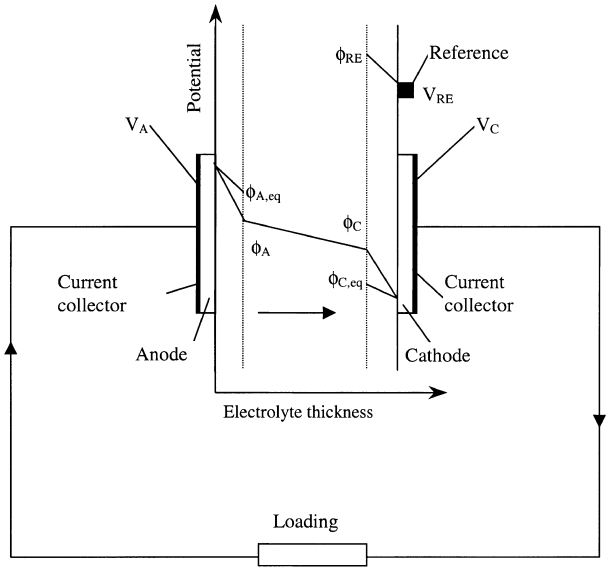

Fig. 1. Potential variation within the electrolyte.

From Figure 1, it can be seen that the terms $(\phi_{A,eq} - \phi_A)$ and $(\phi_C - \phi_{C,eq})$ are the driving forces for the charge transfer at the electrode–electrolyte interface for the anode and cathode, respectively, while the term $(\phi_A - \phi_C)$ is the driving force for oxygen ion transport across the electrolyte. Thus, the 'measured' overpotentials of the electrodes referred to the reference electrode are:

$$\eta_{C,obs} = \phi_{RE} - \phi_C \tag{11}$$

$$\eta_{A,obs} = \phi_A - \phi_{RE} \tag{12}$$

$$\eta_{C,app} = (\phi_{RE} - \phi_C) - (\bar{\phi}_{RE} - \bar{\phi}_C) \tag{13}$$

$$\eta_{A,app} = (\phi_A - \phi_{RE}) - (\bar{\phi}_A - \bar{\phi}_{RE}) \tag{14}$$

where the subscript 'obs' stands for observed overpotential without ohmic compensation, 'app' stands for apparent overpotential with ohmic compensation, $\bar{\phi}$ is the absolute inner potential of the electrolyte under primary distribution conditions, which, in actual measurement, can be obtained by the current interruption technique or impedance spectroscopy.

Equations 11–14 show that the overpotentials of both cathode and anode (for the cases of with and without ohmic compensation) are expressed in terms of absolute inner potentials of the electrolyte. These absolute inner potentials of the electrolyte are readily obtainable by solving the Laplace equation with the prescribed boundary conditions. With boundary conditions of Equations 5–7, the potentials $\bar{\phi}_A$, $\bar{\phi}_C$ and $\bar{\phi}_{RE}$ under primary potential distribution, and with boundary conditions of Equations 8–10, the potentials ϕ_A, ϕ_C and ϕ_{RE}, are all obtained. These simulated results can be used to represent the 'measured' overpotentials with the objective of identifying errors in the measurement due to the effect of current and potential distributions in the electrolyte.

In SOFC, a single cell consists of five layers, that is, current collector–anode–electrolyte–cathode-current collector. Before conducting the modelling of current and potential distributions in the electrolyte, the following assumptions were made: (i) resistance between the current collector and electrode is negligible; (ii) catalyst activity is identical and well-distributed over the electrode; (iii) charge transfer processes follow linear kinetics, which is experimentally justified for SOFC electrode under operating conditions; and (iv) Coaxial disc electrodes are used in this study, which simplify a three-dimensional model with $i(x,y,z)$ and $\eta(x,y,z)$ to a two-dimensional $i(r,z)$ and $\eta(r,z)$. Under these assumptions, the relationship between the overpotential and output current density of the working electrode can be established from the computed current and potential distributions in the electrolyte. Table 1 gives some typical geometric and property parameters of the fuel cell used in the model solved by the finite difference method.

Table 1. Typical geometric and property parameters of a fuel cell

Operating temperature/K	1273
Thickness of electrolyte/cm	0.1
Area-specific polarization resistance of anode/Ω cm^2	0.2
Area-specific polarization resistance of cathode/Ω cm^2	0.2
Resistivity of electrolyte/Ω cm	10
Radius of anode/cm	0.5
Radius of cathode/cm	0.5
Radius of electrolyte/cm	1

3. Results and discussion

All results were calculated from the model assuming that the electrodes are all coaxial. The terms 'symmetrical' and 'asymmetrical' cells mean that the cells under consideration are with identical and nonidentical electrode diameters, respectively. In addition, the word 'measured' means simulated measurement.

The comparison of measured overpotentials with assumed overpotentials of the anode and cathode, for both symmetric and asymmetric cell configurations are shown in Figures 2 and 3, respectively. In the symmetric configuration, the measured overpotential without ohmic loss compensation is underestimated for the anode, but overestimated for the cathode. However, with ohmic loss compensation, the measured overpotentials, for both the cathode and anode, are very close to their respective assumed values, which implicitly means that it is possible to measure accurately the kinetic parameters of the SOFC electrode provided that the reference electrode is properly located. However, in the asymmetric configuration, the measured overpotentials deviate more from the assumed overpotentials than those in the symmetric configuration. With the ohmic loss compensation, there are still significant differences between the measured and assumed overpotentials. In this case, the current interruption or impedance spectroscopy is not

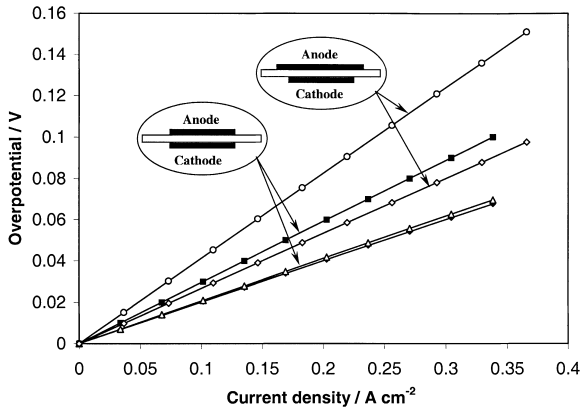

Fig. 2. Overpotential curves at cathode. (◆) Assumed overpotential curve; (■) overpotential curve of symmetric cell without ohmic compensation; (△) overpotential curve of symmetric cell with ohmic compensation; (○) overpotential curve of asymmetric cell without ohmic compensation; (◇) overpotential curve of asymmetric cell with ohmic compensation.

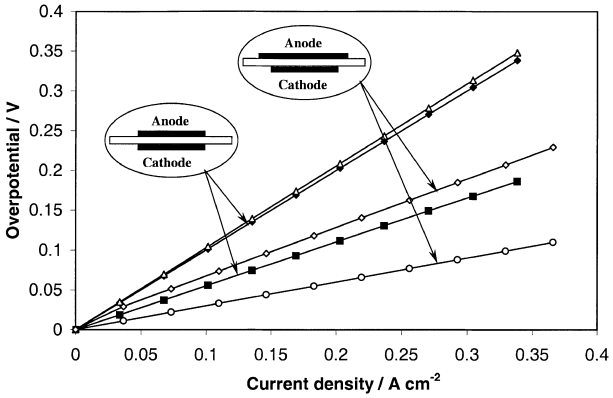

Fig. 3. Overpotential curves at anode. (◆) Assumed overpotential curve; (■) overpotential curve of symmetric cell without ohmic compensation; (△) overpotential curve of symmetric cell with ohmic compensation; (○) overpotential curve of asymmetric cell without ohmic compensation; (◇) overpotential curve of asymmetric cell with ohmic compensation.

useful to compensate the ohmic drop between the reference and working electrodes.

The current density and potential distributions in the electroytes of both the symmetric and asymmetric cells are shown in Figure 4. In the symmetric configuration, the equipotential curves are symmetrically arranged in both the primary and secondary distribution except for the equipotential at the centreline of the electrolyte. If the reference electrode is located at a distance longer than three times the thickness of electyrolyte measured from the edge of the cathode, the potential of the reference electrode will be close to the potential in the centreline of the electrolyte. With this reference electrode arrangement, the electrode overpotentials can be measured with improved accuracy as shown in Figures 2 and 3. However, in the asymmetric configuration, when the radius of the anode is greater than that of the cathode ($r_A > r_C$), the equipotential curves show the tendency of inclining towards the cathode side. Thus, the potential of the reference electrode, if located far away from the cathode edge, approaches the potential of the anode causing overrated (positive deviation) cathode overpotential and underrated (negative deviation) anode overpotential. The current density at the cathode edge increases from 1.96 times the average current density for the symmetric configuration to 2.35 times the average current density for the asymmetric configuration under the primary distribution. Under polarization conditions, the current density distribution trends to be more uniform for both the symmetric and asymmetric configurations. Due to the nature of equipotential curve distribution in the electrolyte and its effect on the potential of the reference electrode, the anode ohmic loss will be overestimated whereas the cathode ohmic loss will be underestimated.

Keeping the size/radius of cathode ($r_C = 0.5$ cm) unchanged, Figures 5 and 6 show the effect of the anode radius (from $r_A = 0.6$ to 0.8 cm) on the measured overpotentials with ohmic loss compensation of the

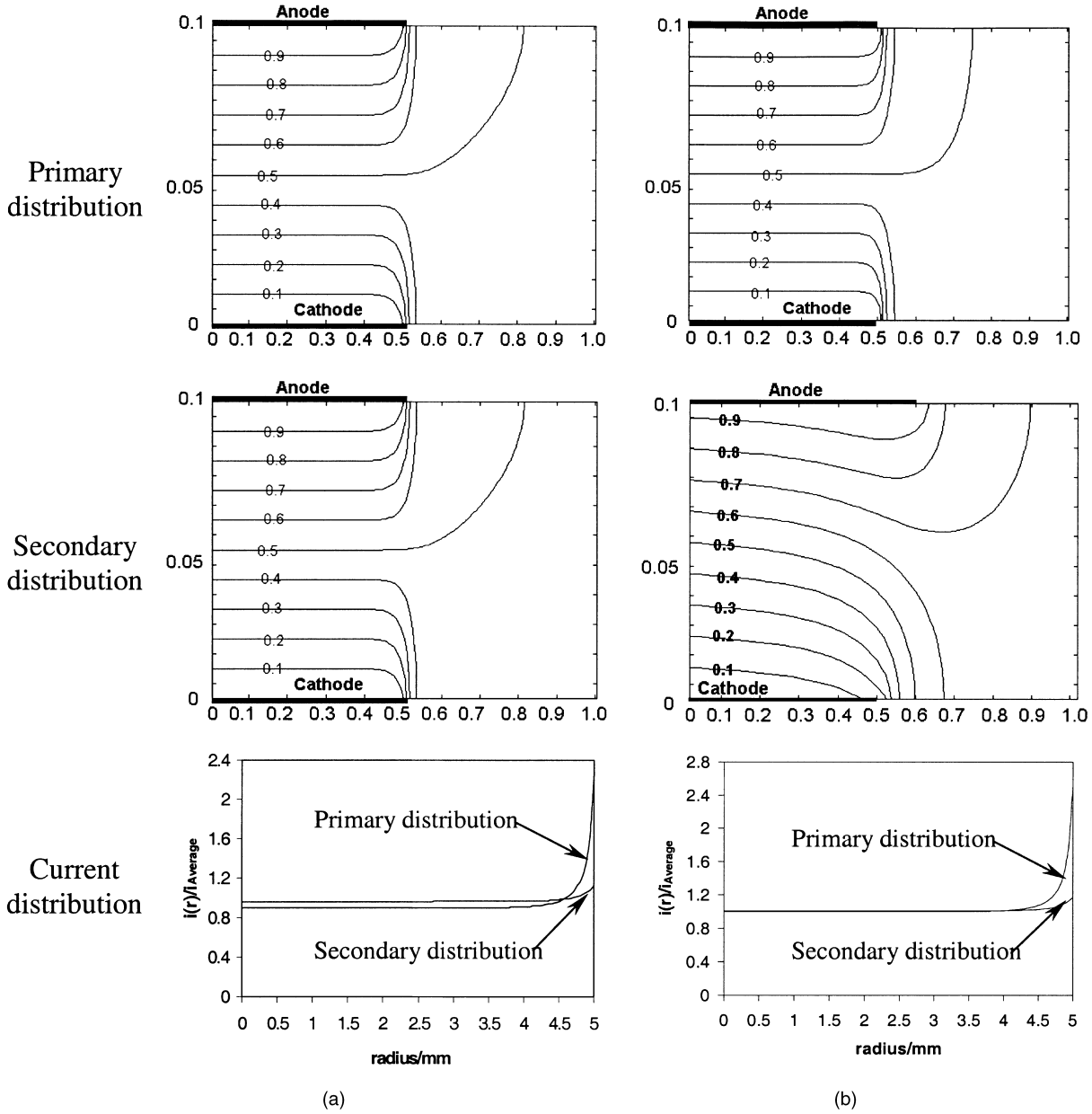

Fig. 4. Potential and current distribution within the electrolyte at cathode side. (a) Symmetric cell configuration; (b) asymmetric cell configuration.

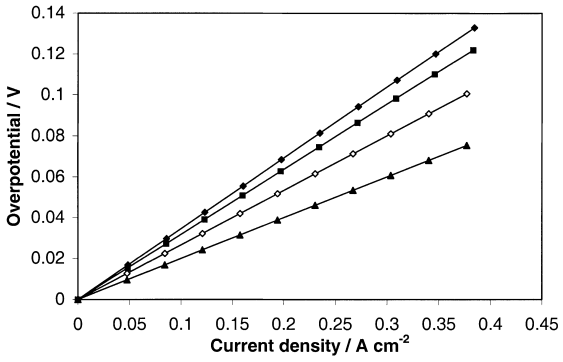

Fig. 5. Overpotential curves of cathode as a function of anode radius. (◇) $r_A = 0.6$ cm; (■) $r_A = 0.7$ cm; (◆) $r_A = 0.8$ cm; (▲) assumed overpotential.

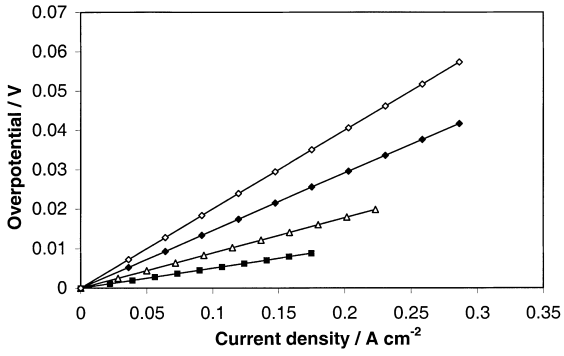

Fig. 6. Overpotential curves of anode as a function of anode radius. (◆) $r_A = 0.6$ cm; (△) $r_A = 0.7$ cm; (■) $r_A = 0.8$ cm; (◇) assumed overpotential.

cathode and anode, respectively. The reference electrode is located at the circumference of the electrolyte disc on the cathode side, which is five times the thickness of the electrolyte measured from the cathode edge. Results show that the measured cathode overpotential deviates from the assumed overpotential and the value is increased with increase in anode radius, which means that the measurement errors introduced by the asymmetric configuration of the electrodes is increased with increase in anode radius. The reverse trend is seen for the anode overpotential, showing that the larger the anode radius, the lower the measured anode overpotential will be. From the overpotential curves of this asymmetric cell, the difference between the measured and assumed anode overpotential is always equal to the difference between the measured and assumed cathode overpotential under the same current density. That is,

$$\eta_{A,a} - \eta_{A,app} = \eta_{C,app} - \eta_{C,a} \tag{15}$$

This means that although error is introduced to the measured anode and cathode overpotentials in the asymmetric cell configuration, the total electrode polarization is not affected.

It should be noted that when the overpotential of the electrode is lower than 0.1 V, the Bulter–Volmer equation could be simplified to give a linear relationship between the current density and electrode overpotential. In addition, the apparent area-specific resistance could be obtained from the slope of the overpotential curve. Determination of electrode resistance based on Equations 28, 29 and 3 may cause some error when the local current density at the working electrode surface is non-uniform. The difference between the computed polarization resistance and the assumed electrode resistance is the source of the error. In percentage terms this is defined as

$$\text{Error } = \frac{R^{A}_{app} - R^{A}}{R^{A}} \times 100 \tag{16}$$

Again, keeping the size of the cathode unchanged ($r_C = 0.5$ cm), Figure 7 shows the effect of the anode radius on the measurement error as a function of the electrolyte thickness. For the symmetric cell configuration ($r_A = r_C = 0.5$ cm), the polarization resistance can be measured quite accurately, in particular for very thin electrolyte. However, for the asymmetric electrode configuration, the measurement error decreases rapidly to a minimum point with increasing electrolyte thickness and then increases slightly with further increase of electrolyte thickness. The thickness corresponding to minimum error is increased with increase in anode radius. Analysis of cell configuration parameters shows that the measurement error is mainly contributed by two factors, one is the ratio of the electrode deviation ($\Delta_{electrode} = r_A - r_C$) to the electrolyte thickness (d_e), and the other is the ratio of the electrode polarization resistance (R^A) to the electrolyte resistance (d_e/σ_e). With the increase in electrolyte thickness, the asymmetric effect on the measurement error weakens and the electrolyte resistance dominates the whole cell performance, causing the tendency of the measurement error as shown in Figure 7.

The dependence of the area-specific polarization resistance on the measurement error as a function of the electrolyte thickness is shown in Figure 8. The radius of the electrode in this study is 0.5 and 0.6 cm for cathode and anode, respectively. The trends of the measurement error are similar to those shown in Figure 7. Because the electrolyte resistance is to be dominant with decreasing electrode polarization resistance, the measurement error increases in such a manner. With increase in electrolyte thickness, the dominant factor shifts from $\Delta_{electrode}/d_e$ to $R^A/(d_e/\sigma_e)$. The electrolyte thickness corresponding to minimum measurement error does not seem to vary much with different area-specific polarization resistance. Combining with the results of Figure 7, one can conclude that the electrolyte thickness corresponding to minimum measurement error of the electrolyte is mainly affected by the deviation of electrode sizes and is non-sensitive to the electrode polarization resistance. Thus, the electrolyte thickness of a fuel cell used for reaction kinetic investigation should be carefully considered to minimize the measurement error. In general, it is desirable to

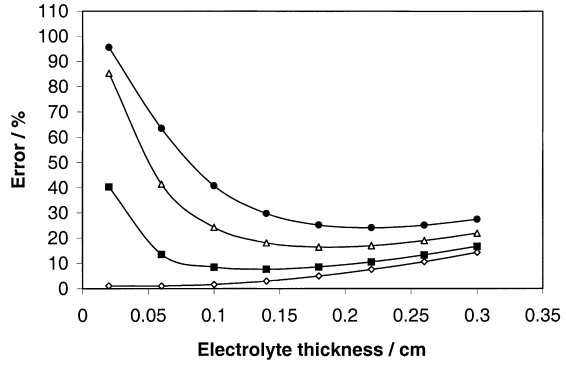

Fig. 7. Dependence of measurement error of cathode on the electrolyte thickness. (◇) $r_A = 0.5$ cm; (■) $r_A = 0.52$ cm; (△) $r_A = 0.56$ cm; (●) $r_A = 0.6$ cm.

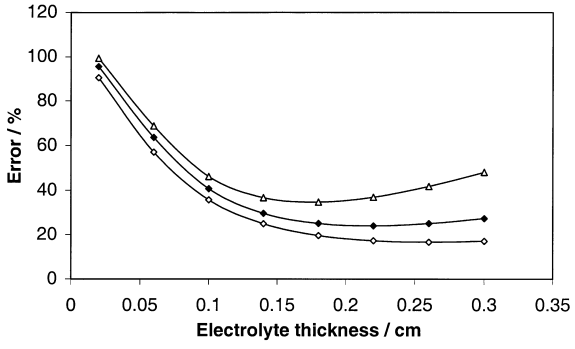

Fig. 8. Effect of specific polarization resistance on the cathode. (△) $r_A = 0.6$ cm; $r_A = r_C = 0.1\ \Omega\ cm^2$; (◆) $r_A = 0.6$ cm, $r_A = r_C = 0.2\ \Omega\ cm^2$; (◇) $r_A = 0.6$ cm, $r_A = r_C = 0.4\ \Omega\ cm^2$.

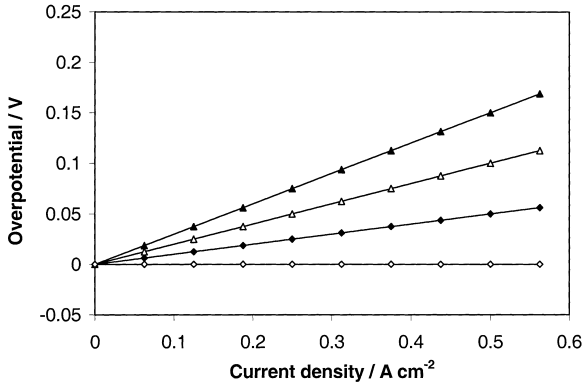

Fig. 9. Measured overpotential curves of anode-support fuel cell. (◆) Assumed anode overpotential; (△) assumed cathode overpotential; (▲) measured cathode overpotential; (◇) measured anode overpotential.

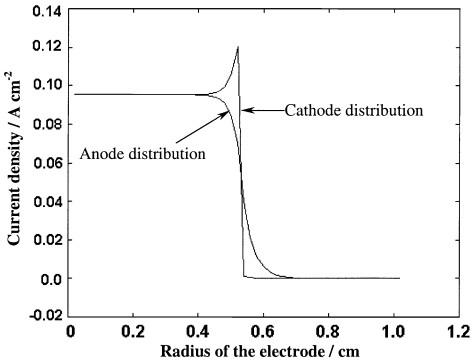

Fig. 10. Current distribution at anode and cathode surface of anode-support fuel cell.

design a cell with thick electrolyte, in particular for an asymmetric cell.

When studying the effect of electrode deviation on the measurement error, one special case has been considered, that is, the anode-supported cell where the anode radius is equal to the electrolyte radius. Assuming the polarization resistance of the anode and cathode to be 0.1 and 0.2 Ω cm^2, respectively, Figure 9 shows that the measured anode overpotential is almost equal to zero and the measured cathode overpotential is equal to the sum of the assumed anode and cathode overpotentials. Figure 10 shows the anode and cathode current density distributions of the anode-supported cell. Results show that the current density of the cathode at the edge is higher than that at the cathode centre point, while the current density of the anode decreases along the anode radius. Since there is no reaction in the anode at radius greater than 0.7 cm, the overpotential of the anode should be equal to zero. Therefore, for the anode-supported fuel cell, the potential of the reference electrode, at a distance equivalent to three times the electrolyte thickness measured from the cathode edge, will be equal to the equilibrium potential of the electrolyte at the anode–electrolyte interface. It is impossible to distinguish the source of polarization contributed either from the anode or cathode.

4. Conclusions

The simulated measurement showed that the measurement accuracy of the electrode polarization is influenced by the parameters that have impact on the potential distribution in the electrolyte. These parameters include electrode deviation, electrolyte thickness and electrode polarization resistance. The cell geometrical configuration should be carefully designed to accurately determine the electrode overpotential in a three-electrode measurement system. In this study, the following conclusions can be stated:

(i) In a symmetric electrode arrangement, measurement of electrode overpotential can be improved by ohmic loss compensation. Although the current interruption method or impedance spectroscopy can be employed to compensate/correct the measurement error for the symmetric electrode system, it is not useful when dealing with asymmetric electrode systems.

(ii) If the anode radius is greater than the cathode radius ($r_A > r_C$) in a three-electrode system, the measured cathode overpotential will be overestimated while the measured anode overpotential will be underestimated. This is due to the potential of the reference electrode approaching the potential of the anode with shift from primary to secondary distribution.

(iii) Although the measured cathode overpotential is increased with increase in anode radius, and the measured anode overpotential is decreased with increase in anode radius, the total electrode overpotential of the cell remains unchanged.

(iv) The measurement error of polarization resistance in a three-electrode system is related to the anode radius, electrolyte thickness and electrode polarization resistance. The electrolyte thickness corresponding to minimum measurement error is increased with increase in anode radius and is non-sensitive to the electrode polarization resistance.

(v) In an anode-supported fuel cell, because the potential of the electrolyte outside the reference electrode diffusion double layer (ϕ_{RE}) is equal to the potential of the electrolyte just outside anode diffusion double layer (ϕ_A) under equilibrium conditions, it is impossible to distinguish the source of polarization contributed by either the anode or cathode.

References

1. H. Fukunage, M. Ihara, K. Sakaki and K. Yamada, *Solid State Ionics* **86–88** (1996) 1179.
2. H. Uchida, N. Mochizuki and M. Watanabe, *J. Electrochem. Soc.* **143** (1996) 1700.
3. M. Watanabe, H. Uchida and M. Yoshida, *J. Electrochem. Soc.* **144** (1997) 1739.
4. J. Newman, *J. Electrochem. Soc.* **113** (1966) 1235.
5. A.C. West and J. Newman, *J. Electrochem. Soc.* **136** (1989) 139.

6. A.C. West and J. Newman, *J. Electrochem. Soc.* **136** (1989) 3759.
7. M. Nagta, Y. Itoh and H. Iwahara, *Solid State Ionics* **67** (1994) 215.
8. J. Winkler, P.V. Hendriksen, N. Bonanow and M. Mogensen, *J. Electrochem. Soc.* **145** (1998) 1184.
9. T. Kato, A. Momma, Y. Kaga, S. Nagata, Y. Kasuga and M. Kitase, *Solid State Ionics* **132** (2000) 287.
10. S.B. Adler, B.T. Henderson, M.A. Wilson, D.M. Taylor and R.E. Richards, *Solid State Ionics* **134** (2000) 35.
11. P. Costamagna, P. Costa and V. Antonucci, *Electrochim. Acta* **43** (1998) 375.
12. A.J. Bard and L.R. Faulkner, 'Electrochemical Methods' (J. Wiley & Sons, New York, 2001).